MODELING ELECTROPHYSIOLOGICAL DYNAMICS IN TRANSIENT DEEP BRAIN STIMULATION OF THE SUBCALLOSAL CINGULATE

A Thesis
Presented to
The Academic Faculty

by

Liangyu Tao

In Partial Fulfillment
of the Requirements for the Degree
Bachelors of Science in the
School of Biomedical Engineering

Georgia Institute of Technology
May 2017

MODELING ELECTROPHYSIOLOGICAL DYNAMICS IN TRANSIENT DEEP BRAIN STIMULATION OF THE SUBCALLOSAL CINGULATE

Approved by:

Dr. Robert J. Butera, Advisor
School of Biomedical Engineering
Georgia Institute of Technology

Dr. Garrett B. Stanley
School of Biomedical Engineering
Georgia Institute of Technology

Date Approved: May 5, 2017

ACKNOWLEDGEMENTS

I would like to thank my parents and brother for their endless faith and support. I would also like to thank graduate student advisor Vineet R. Tiruvadi (MD PhD candidate) for invaluable assistance with modeling assistance, guidance in interpreting clinical significance, and both personal and professional development over the latter half of my undergraduate career. I would also like to thank graduate students Riley Z. Townson (Georgia Institute of Technology) and Rehman Ali (Stanford University) for giving me feedback on model interpretation and professional development. Finally, I would like to thank Dr. Robert Butera for his mentorship and support of the ongoing research.

TABLE OF CONTENTS

LIST OF FIGURES

LIST OF ABBREVIATIONS

MDD	Major Depressive Disorder
TRD	Treatment-Resistant Depression
DTI	Diffusion Tensor Imaging
SCC	Subcallosal Cingulate
LFP	Local Field Potential
HAM-D	Hamilton Depression Rating Scale
ETC	Electroconvulsive Therapy
DTI	Diffusion Tensor Imaging
SCCwm	SCC White Matter Tract
EEG	Electroencephalogram
ISI	Interspike Interval
GABA	*gamma*-Aminobutyric acid
GUI	Graphical User Interface
STFT	Short Time Fourier Transform
API	Application Program Interface

LIST OF SYMBOLS

E	Population of Excitatory Subpopulation Fire
I	Population of Inhibitory Subpopulation Fire
r, k	Arbitrary Constants for Wilson Cowan Model
m_{ij}	Weighted Connectivity Matrix
w_{ee}	Excitatory Subpopulation Self Excitation
w_{ie}	Inhibition of Excitatory Subpopulation by Inhibitory Subpopulation
φ_E, φ_I	Threshold of Fire for Excitatory and Inhibitory Subpopulations
θ_E, θ_I	External Stimulus Applied Directly to Wilson Cowan Populations
τ_E, τ_I	Firing Rate Constants for Excitatory and Inhibitory Subpopulations
τ	Ratio of Excitatory to Inhibitory Firing Rate Constants
σ_s	Saddle Node Eigenvalue
λ_1, υ_1	Real and Imaginary Components of Eigenvalue

SUMMARY

Deep brain stimulation (DBS) is a promising investigational treatment for patients with treatment resistant depression (TRD). However, the exact mechanism of action of SCCwm-DBS is unknown and its effects on the electrophysiology of brain networks are poorly understood despite high clinical efficacy.

Recent hardware advances have enabled stimulation and recording in clinical populations. Local field potentials (LFPs) recorded from patients under transient stimulation demonstrate strong oscillatory features that change over time. Three scales are explored in order to understand the network-level contributions to chirp generation. It was found that a single Wilson Cowan population could generate a transient down chirp when the parameters are near a homoclinic bifurcation. In a network of Wilson Cowan models informed by network connections seen in diffusion tensor imaging (DTI) of SCCwm-DBS and connected via glutamatergic excitatory-excitatory connection, a modeled stimulation on the connections between regions showed the appearance of transient down chirps in Wilson Cowan populations downstream from the populations directly connected by the edge of excitation. The further addition of inhibitory connections between Wilson Cowan populations showed more consistent appearances of transient down chirps in the modeled right temporal pole, a feature which suggests an importance of future LFP recordings from the temporal lobe.

The results of this thesis will be used to interpret empirical data collected from patient populations and can be objectively validated in patients through future experiments. The larger implications of this work may lead to identification of electrophysiological biometrics of SCCwm-DBS targeting and efficacy.

CHAPTER 1

INTRODUCTION

Major Depressive Disorder (MDD) is highly debilitating major mood disorder characterized by five or more symptoms including thoughts of death, insomnia, changes in weight, and feelings of hopelessness among other symptoms for a continuous period of two or more weeks (American Psychiatric Association, 2013). Treatment Resistant Depression (TRD) is a subset of MDD characterized by the failure to respond to four different types of antidepressant treatments (Fava, 2003; Nobler et al., 2001). Current metrics of testing for TRD response involve utilizing scoring methods such as a Hamilton Depression Rating Scale (HAM-D) to test for efficacy of both antidepressant drugs and more invasive methods such as electroconvulsive therapy (ETC) and deep brain stimulation (DBS). Current clinical treatment strategies proceed empirically but more targeted neuromodulation therapies are showing strong promise in treating MDD. The aim of our research group is to explore the mechanisms of DBS action in treating TRD.

Clinical trials in DBS of the white matter tracts near the subcallosal cingulate (SCC), or SCCwm, at 130 hz stimulation had shown significant and continued patient response over the course of two years (Mayberg et al, 2005). Diffusion tensor imaging (DTI) images with whole brain tractography have established a network of brain regions and their connecting white matter tracts associated with successful TRD recovery in DBS. These pathways involve the connection of the SCC to the Medial Frontal cortex via forceps minor and uncinate fasciculus, the connection of the Rostral and dorsal cingulate cortex via the cingulum bundle and the connection of the SCC to the Subcortical Nuclei

(Riva-Posse et al, 2014). Recent advances in hardware have enabled recordings of Local field potentials (LFP) from the brain region being targeted. These LFP recordings before, during, and following DBS with Medtronic's Activa PC+S DBS system have shown the appearance of dynamic changes in electrophysiological patterns. The most notable of these is the appearance of transient down chirps, a decrease in LFP frequency over time, during the first 20-100 seconds of stimulation (Figure 1). These down chirps are a patient specific, reproducible, response seen in the SCC LFP that may help to constrain neural circuit dynamics impacted by DBS, and be used as a metric to assess SCC neurophysiology. Although DBS of TRD has been shown to be a promising investigational treatment method for TRD, the mechanisms governing patient response and the generation of these transient down chirps are not well understood.

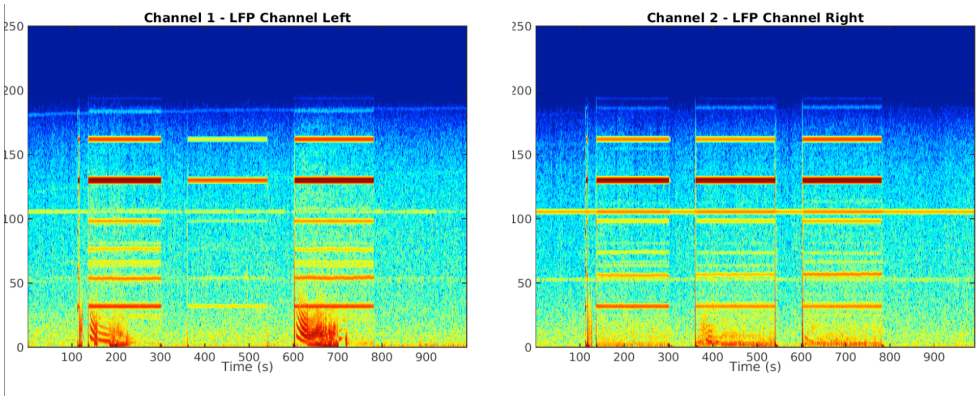

Figure 1. Local Field Potential Recordings of SCCwm These empirical spectrograms showing left and right SCC LFP recordings during DBS. Left SCCwm tract stim occurs at 110 seconds, Right SCCwm tract stim occurs at 360 s, Bilateral SCCwm tract stim occurs at 600 s. Transient down chirps can be seen in left LFP recordings following left and bilateral SCCwm tract stim and in right LFP recordings following right and bilateral SCCwm tract stim.

This thesis aims to develop a model that can be used to infer the underlying excitatory-inhibitory activity that gives rise to dynamic oscillatory features such as the

transient down chirps. Specifically, this paper will focus on the generation of the aforementioned transient down chirps via a single region and a network level mean field population-firing model. A network level model informed by tractography is necessary as DBS is thought to directly modulate a network of brain regions (McIntyre & Hahn, 2010). In the case of SCCwm-DBS, stimulation is known to modulate a network of brain regions (Mayberg, 2009). Despite this, the possibility of being able to explain these recordings with lower level single region dynamics cannot be ignored. Based on these observations and concerns, I conducted an incremental approach to this problem.

I begin by using a mean field approach to model a single isolated brain region. A biophysical mean field model would allow for a generalization of the response without knowing the neuron or ion level composition of the modeled brain region, something clinically challenging to do. A Wilson Cowan model (Wilson & Cowan, 1972) was chosen, as it is a simple mean field biophysical model, which can show a wide variety of oscillatory dynamics. Furthermore, since its first introduction, the Wilson Cowan model has been extended to include defined energy functions under cases of symmetric connectivity (Hopfield & Tank, 1986), spike-frequency adaptation and bursting (Soula & Chow 2007), among others. This allows ease of future incorporation of extensions to explain critical variances unable to be explained by the base Wilson Cowan model. As this model looks at excitatory and inhibitory population dynamics within a single population, this one population model would help understand possible localized mechanisms of action following SCCwm-DBS.

I then introduce a two-brain region model designated by a system of two connecting Wilson Cowan populations. DTI recordings show a forceps minor connection

between the left and right SCC, regions where LFP recordings elicit transient down chirps following SCCwm-DBS (Riva-Posse et al, 2014). Studying a two population Wilson Cowan model can provide possible regional mechanisms of action of this the forceps minor connection as well as give an understanding on how connecting Wilson Cowan populations can generate the down chirp seen in SCCwm-DBS. Past research has been conducted on the dynamics of these two regions and cables of Wilson Cowan models in the context of modeling epileptical behavior (Meijer et al, 2015). However, there has not been a characterization of chirp generation in the two-region Wilson Cowan models.

After understanding the dynamics of chirp generation in this two-region model, I expanded the Wilson Cowan model into a network of Wilson Cowan models. DTI shows that precise stimulation of four white matter tracts is needed to alleviate depression. The brain regions connected by these white matter tracts are likely targets of direct electrophysiological modulation. A subset of these regions is measurable using both invasive DBS LFP recordings and noninvasive scalp electroencephalogram (EEG). Six brain regions, in particular are hypothesized to be directly modulated by precise SCCwm-DBS. The six-node network of Wilson Cowan models detailed in this work is directly informed by the tractography of an ongoing patient-based study. The use of this model allows for the prediction of possible acute transient level responses to DBS of SCCwm tracts. The model is topologically informed by the proposed SCC circuit and shows the impact of topological connections in the generation of clinical LFP data.

While there are other much more complex models in the literature (Moran et al., 2007; Sanz-Leon et al., 2015), the creation of a simple, fast model which can capture the

general dynamics and important variance of the physiological changes caused by DBS of TRD patients will allow for ease of future integration of a prediction and analysis tool into a real time, closed loop DBS device. Furthermore, Neural Mass and other forms of more complex mean field models have been able to show the onset of chirps under certain excitatory, inhibitory balances (McCarthy et al., 2011; Froemke, 2015). However, if a simple mean field model based on the SCC network can produce these chirps via a similar mechanism of excitatory, inhibitory balance, then clinically, it may be possible to make directed hypothesis testing that can be tested in patients with excitatory/inhibitory blockers.

I end with the development of a graphical user interface (GUI) and toolbox, which allows for clinical investigators to generate and conduct analysis on the network Wilson Cowan model. Development of a toolbox capable of generating and predicting the appearance of possible electrophysiological biomarkers such as the transient down chirps seen in clinical settings can ultimately allow for clinicians to better monitor TRD and conduct analysis with real time LFP data.

This work is important because it will allow for a quantitative description of an empirical electrophysiological feature and possible biometric for SCCwm-DBS efficacy. Furthermore, this work can be used to hypothesis test clinically feasible experimental procedures within the bounds of model based hypothesis testing. The focus of the network modeling effort is to understand how the topology affects chirp features. If a direct connection can be modeled between connectivity changes and chirp features, inversion of the model will be a next step to possibly infer the connectivity changes that are being induced by SCCwm-DBS stimulation conditions that give rise to the chirp.

Ultimately, a network model with tuned parameters and hypothesized structures based on the SCC circuit will be useful both in describing the mechanism of the signaling between the white matter tracts of interest and in predicting responses from stimulation parameters not yet tested via clinical trials.

CHAPTER 2

METHODOLOGY

Modeling a complex system must begin at a scale representative of the system. LFP and EEG recordings measure mesoscopic brain dynamics that are representative of large numbers of synchronous neurons firing in a similar spatial orientation (Buzsaki, 2006). These recorded oscillations are important because these oscillations may have of characteristic frequency ranges, spatial distributions, and patterns such as the transient down chirps seen in SCCwm-DBS. Understanding and modeling these patterns can give us insight into the underlying neuronal networks that generate these oscillations. Given the nature of the composition of these electrophysiological recording methods, a mean field population modeling approach is an appropriate set towards modeling the underlying neuronal networks and their dynamics that may cause these empirically measured recordings. Mean field models allow for the application of dynamical analysis methods such as bifurcation analysis to be conducted directly to a network of neurons, which allows for analysis of these mesoscopic brain dynamics. In addition, mean field neural mass models have been used heavily in studying the electrophysiological dynamics in other disorders, being capable of generating beta frequency dynamics seen in Parkinson's disease patients (McCarthy, et al., 2011) and high-frequency, chirp-like signatures observed in EEG signals recorded in epileptical patients (Molaee-Ardekani, et al., 2009). Furthermore, mean field neuron models allow for a top down approach where further complexity may be added to a general model in explaining more of the complex system as needed. In this thesis, a simple mean field population model scaled from one

population to six populations connected together in an network inspired by patient tractography will be explored. Finally, the parameters of these mean field models relate directly to excitatory and inhibitory processes in neuronal tissue. These processes have been hypothesized and shown to be able to explain various types of electrophysiological dynamics seen in similar diseases treatable by DBS (McCarthy, et al., 2011; Froemke, 2015).

The mean field model used for a population of neurons was the Wilson Cowan model. A Wilson Cowan population is composed of an excitatory and an inhibitory subpopulation. Each of these subpopulations represents large numbers of firing neurons whose cohesive firing pattern can contribute to the mesoscopic oscillations we are trying to model.

This model was solved in MATLAB using a modified Runge-Kutta differential equation solver. The local field potential of a region was modeled as the weighted sum of the excitatory and inhibitory subpopulation activities from each Wilson Cowan population. Dynamical systems analysis methods such as phase plane and eigenvalue analysis were conducted on the single population Wilson Cowan model. Eigenvalue and bifurcation analysis were conducted for both the two-population model and the topologically guided model. Spectrograms were generated for all model outputs to show the change in frequency over time of the modeled signal.

Modeling

Computational modeling is an useful tool to simulate and accelerate the study of possible mechanisms of action in biological and other real world systems, like that of

DBS of TRD patients. In the case of DBS of TRD patients, a network of mean field biophysical models can be used to understand the dynamics of groups of neurons that would cause the observed signals in LFP recordings. A group of neurons can furthermore be modeled as a single population of neurons with a subpopulation of excitatory neurons and a subpopulation of inhibitory neurons. The classic example of this mean field approach is the Wilson Cowan model (Wilson & Cowan, 1972).

Wilson Cowan

A network of mean field population models was used to model the dynamics that would cause the observed signals in LFP recordings. Each neural region was modeled as a Wilson Cowan population, consisting of subpopulations of excitatory neurons and inhibitory neurons (1). Due to the simplicity of the neural oscillations elicited in Wilson Cowan models, neural oscillations and stimulus-dependent evoked responses can be easily explored and predicted as to test current hypotheses of DBS action. As Wilson Cowan subpopulations are homogeneous, the excitatory signaling are assumed to be glutamate based and the inhibitory signaling are assumed to be GABA based.

$$\tau \frac{dE}{dt} = -E + (1 - rE) \cdot S_e\left[-k\left(m_{ij} w_{ee} E - w_{ie} I - \varphi_E + \theta_E\right)\right]$$

$$\frac{dI}{dt} = -I + (1 - rI) \cdot S_e[-k(w_{ie} E - w_{ii} I - \varphi_I + \theta_I)]$$

$$\tau = \frac{\tau_E}{\tau_I} \quad (1)$$

The white matter tracts connecting each neural region were modeled by excitatory-excitatory subpopulation connectivity, m_{ij}, between regions (Figure 2). The white matter tracts modeled via the connectivity of neural regions are situated in the

cortex. Many long distance cortical pathways involve excitatory network connectivity. Glutamate was chosen to be modeled as the excitatory neurotransmitter due to the extensive literature on modulation and change in glutamate activity in the cortex (Maddock et al., 2016; Lewis et al., 2003).

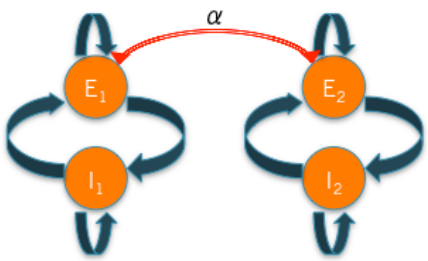

Figure 2. Modeled Excitatory-Excitatory Connections Between Neurons . Connectivity is modeled by α and representing glutamate based excitatory-excitatory action.

Network Topology

The network model was informed by the SCC Circuit shown to be involved in DBS of SCCwm tracts via DTI (Figure 3). In this circuit, the SCC, mF10, and Temporal lobes are connected via the uncinate fasciculus white matter tract. The left and right mF10's are connected via the forceps minor. The left and right SCC are also connected via the forceps minor. Due to this, the weights of the modeled white matter tracts connected via the uncinate fasciculus were assumed to be uniform, but may be different from the forcepts minor. The white matter tracts were modeled via interregional weighted connectivity matrices. The model was explored for connectivity weights in the range of 0.1 to 0.5, with the assumption that network influences will be smaller than intraregional effects on the region's Excitatory/Inhibitory firing population. As DBS was conducted with 130Hz stimulation targeted at SCCwm tracts, stimulation was modeled as first a step

change in network connectivity of proposed location of SCCwm stimulus, and then as a 130hz modulator the SCCwm connectivity. Finally, the neural regions and white matter tracts in each hemisphere is consistent with the counterparts in the other hemisphere.

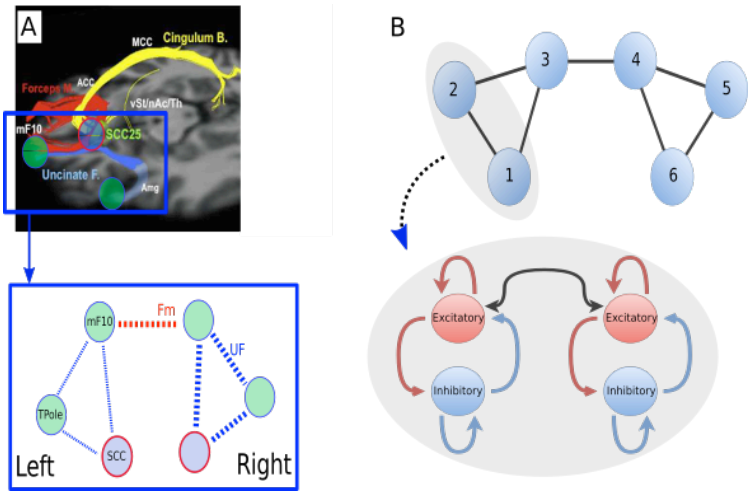

Figure 3. Layout of SCC Network Informed by DTI. Panel A shows DTI tractography indicating SCCwm tracts and neural regions involved in DBS of TRD (Riva-Posse el al, 2014). Panel B shows network model informed by the DTI tractography.

Local Field Potential

In the simplest case, LFP recordings can be represented as a weighted sum of the current outputs of neurons near the recording electrode (Einevoll et al, 2013). Other more representative models for LFPs include microscopic models utilizing the Maxwell equations (Bedard et al., 2004) and macroscopic models utilizing mean field methods (Bédard & Destexhe, 2009). Due to the difficulty of decomposing clinical LFP recordings and the scope of this thesis, LFPs were modeled with a summation of modeled excitatory and inhibitory neural subpopulation responses within a neural region.

Dynamical Modeling Metrics

Phase Plane Analysis

The phase plane of a one-population system could be visualized by plotting the amount of excitatory activation by the amount of inhibitory activation. The resulting trajectory could be used to find limit cycles and stability within a two dimensional system. Nullclines were further solved and plotted to break up the phase space into various regions of qualitative behavior. The following equations were used to solve for the nullclines (2).

$$0 = -E + (1 - rE) \cdot S_e[-k(w_{ee}E - w_{ie}I - \varphi_E + \theta_E)]$$
$$0 = -I + (1 - rI) \cdot S_e[-k(w_{ie}E - w_{ii}I - \varphi_I + \theta_I)] \quad (2)$$

Eigenvalue Analysis

Eigenvalues can be used to solve for stability and bifurcations in dynamical systems. In the simplest case, a positive eigenvalue will result in an unstable system and a negative eigenvalue will result in a stable system. When the eigenvalue is negative, then the system will reach a cyclical oscillation (limit cycle). In the case of a homoclinic bifurcation, there must be a saddle node with eigenvalues that must satisfy one of the following criterions:

1. The leading eigenvalues of a saddle node are real and simple; $\mu_1 < 0 < \lambda_1$
2. The leading stable eigenvalues are real and simple; the leading unstable eigenvalues are imaginary and simple
3. The leading eigenvalues are non-real and simple.

Where leading eigenvalues are those that are closest to the imaginary axis. The saddle node quantity was defined as $\sigma_s = Re(\lambda_1) + Re(\mu_1)$. Where λ_1 is defined as the leading

unstable eigenvalue and μ_1 is defined as the leading stable eigenvalue. In the real and symmetric case, the Jacobi eigenvalue algorithm was used to solve for the eigenvalues. In the nonsymmetrical or non-real case, the power iteration was used.

Bifurcation Analysis

Many dynamical systems, such as the Wilson Cowan model are composed of differential equations. These differential equations involve a number of parameters, which describe various inputs the behavior of the dynamical system. In some cases, a small variation in a parameter can cause a significant impact on the behavior of the dynamical system. The point where the system changes from one type of behavior to another is defined as a bifurcation. In many cases, the changes in the mesoscopic oscillation patterns seen in EEG and LFP recordings may be caused by specific critical changes in input or other factors to the contributing neuron populations, much like a bifurcation.

There are two main categories of bifurcations. Local bifurcations, such as Hoph and Period-doubling bifurcations, occur when the change in parameter causes a change in the stability of the system to change. As an analogy, this can be thought of as if you are driving to the grocer and there has been an accident forcing a detour. Now your trajectory has changed because of a change in your routine system. Global bifurcations, such as homoclinic and heteroclinic bifurcations, occur when the change in parameter causes a trajectory to collide with an equilibrium point (a constant solution), thereby causing a new trajectory to occur. As an analogy, this can be thought of as if you are driving to the

grocer. Suddenly, you see a farmers market up ahead in your trajectory. From then on, you go to the farmers market every week rather than the grocer.

Understanding how, when, and where these bifurcations occur allows the modeler to study and make statements about the modeled dynamical system. In this work, Bifurcation analysis was conducted using the MATLAB software MatCont.

Spectrogram

Brain oscillations are ubiquitous and can be recorded with methods such LFP and EEG (Buzsaki, 2006). Analysis of these oscillations relies heavily on Fourier analysis techniques and decomposition in the frequency-domain. Additionally, given the dynamic nature of brain activities, time-domain analysis and representations are also important. Using techniques such as short time Fourier transform (STFT) allows for a time-frequency domain representation that allows for visualization and analysis across domains.

A spectrogram is a widely used visual representation of the frequencies of signals as they vary over time. Spectrograms were generated using MATLAB spectrogram function, which computes the squared magnitude of the short time Fourier transform using a small window width (3).

$$spectrogram(t, w) = |STFT(t, w)|^2 \tag{3}$$

The window widths were defined to be 128 samples with 120-sample overlap in order to allow for ample sampling without taking large amounts of computational time. The sampling frequency was defined as 1/fs Hz.

CHAPTER 3

RESULTS

To study how a population of neurons can generate the specific electrophysiological signals seen in empirical SCC LFP recordings, I first performed parameter analysis of the single Wilson Cowan model using dynamical systems analysis methods detailed in the methods. Then model was then expanded to two populations to look at how connectivity between regions may affect the dynamical oscillations. Following this, the model was expanded to the topologically informed network model to show possible modeled neuron populations that display transient down chirps. Spectrograms were shown for visualization of time-frequency dynamics.

Section 1: Single Population

A model of the Single Wilson population was generated using MATLAB. A parameter space exploration was conducted to search for possible parameter sets that may generate a transient down chirp. Phase plane portraits of the time course showed a set of parameters that can generate these transient down chirps. One subset of these parameters used was $w_{ei} = 1.5$, $w_{ie} = 1$, $w_{ii} = 0.25$, $w_{ee} = 1$, $\varphi_E = 0.125$, $\varphi_I = 0.4$, $\tau_E = 0.01$s, $\tau_I = 0.0067641$s, $r_E = 0$, $r_I = 0$, $a_E = 50$, $a_I = 50$, $\theta_E = 0$, $\theta_I = 0$ (Figure 4, 5). An extended list of parameters that can elicit the transient down chirp responses can be found in Appendix A, Table 1. Time constants were chosen to be within the bounds of possible time constants for glutamate and GABA based neurotransmitter action. A phase-plane analysis of parameters can be found in Appendix A.

From the time domain, it can be seen that in generating a transient down chirp, the excitatory subpopulation has a 40 percent higher peak firing activity than the inhibitory subpopulation (Figure 4). Furthermore, the end of the transient down chirp occurs following an end of the oscillations for the excitatory and inhibitory subpopulations.

Phase Plane

Phase plane analysis of the transient down chirp shows the appearance of a homoclinic bifurcation. Nullclines shows the appearance of a stable node at E = 0.215, I = 0.4. There is an unstable downstream node at E = 0, I = 0. Finally, there is a saddle point at E = 0.1, I = 0.01. The start of the trajectory must be at an Excitatory/Inhibitory balance encompassed within the homoclinic trajectory. The time trajectory of oscillations will take longer as the phase plane trajectory grows until it reaches the homoclinic bifurcation (Figure 4). This in turn causes a decrease in frequency.

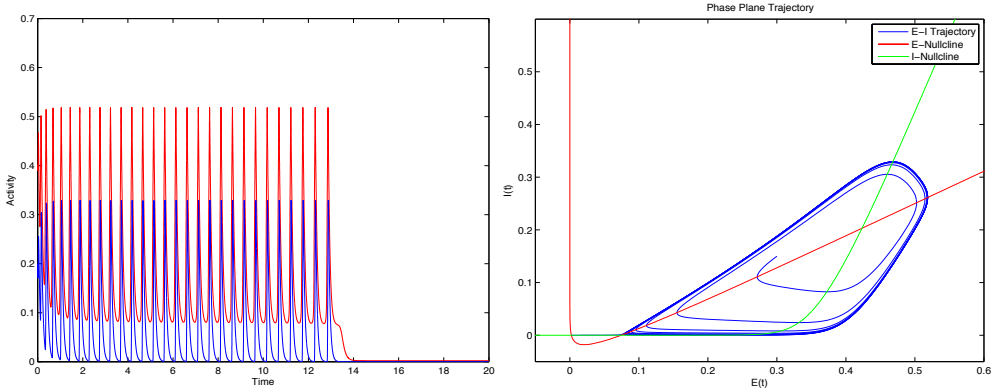

Figure 4. Time Course and Phase Plane of Modeled Down Chirp. Phase plane trajectory show Excitatory/Inhibitory time course where time is implicit. This trajectory shows a homoclinic bifurcation. Initial conditions: E = 0.3, I = 0.15.

Frequency Space

Frequency domain representations of the modeled transient down chirp showed appearance of chirps that lasts upwards of 20 seconds with a maximum frequency of 20 hz. An example of a modeled transient down chirp lasting 13 s and reaching 15 Hz max frequency is show in figure 5 below.

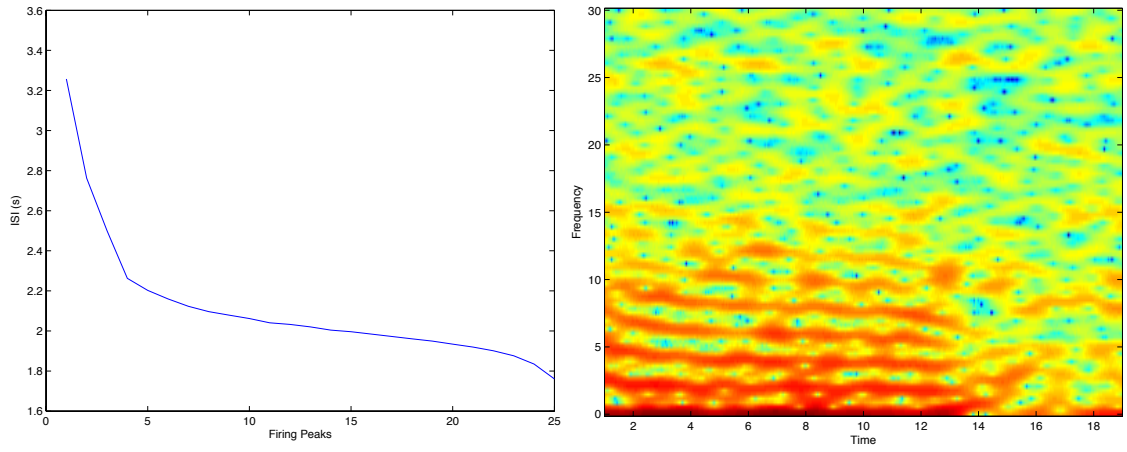

Figure 5. ISI and Spectrogram of Single Population Down Chirp. Left figures shows the Interspike Interval of the fundamental frequency of the transient down chirp and the right figure shows the spectrograms of modeled excitatory and inhibitory population behavior.

Applying time constant constraints of 10 ms for the excitatory glutamergic subpopulation and 6.76 ms for the inhibitory GABA subpopulation, it was found that the resulting response excitatory and inhibitory population response decreased in frequency, but increased in duration. The time constants were chosen to be within range of possible time constants for these neurotransmitters (Computational Neuroscience Research Group@Waterloo, n.d.).

Section 2: Two Populations

We extended the single population model to a two-population model to understand how an excitatory-excitatory connection between two populations of Wilson Cowan models can elicit a chirp. A modulation of the connectivity between the populations was conducted by decreasing the excitatory-excitatory connectivity to 0.03. This was to simulate the condition where stimulation may interrupt connectivity between regions. Figure 6 shows a raster plot of the firing of two Wilson Cowan populations connected with various levels of connectivity. These Wilson Cowan populations were set at parameters of $w_{ei} = 1.5$, $w_{ie} = 1$, $w_{ii} = 0.25$, $w_{ee} = 1$, $\varphi_E = 0.125$, $\varphi_I = 0.5$, $\tau_E = 0.01$s, $\tau_I = [0.0065\text{s}, 0.0074\text{s}]$, $r_E = 0$, $r_I = 0$, $a_E = 50$, $a_I = 50$, $\theta_E = 0$, $\theta_I = 0$. These parameters were set such that it is near a homoclinic bifurcation individually, but still capable of maintaining a stable oscillation. Other parameter sets near homoclinic bifurcations as well as cases where the two Wilson Cowan populations were completely the same were also explored. The general findings were similar across these simulations.

This two-population model showed the appearance of transient down chirps following a sudden decrease in connectivity. Furthermore, results showed the appearance of some inter-population mechanism that may cause the appearance of the down chirp due to differential response to stimulus between regions (Figure 6). It was found that increasing the connectivity between regions past 0.5 caused a general suppression of modeled excitatory and inhibitory firing in both populations.

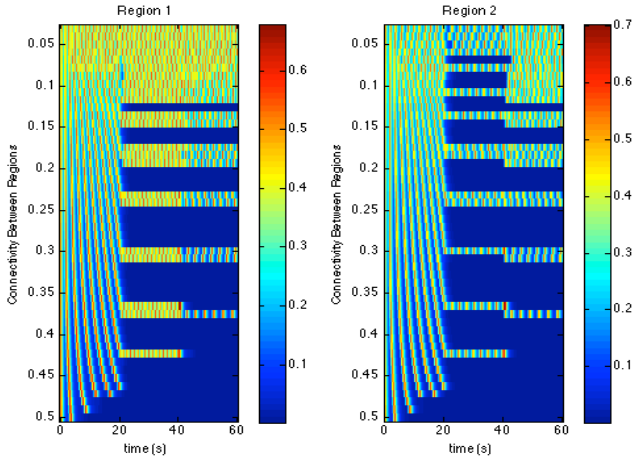

Figure 6. Modeled Raster Plot of Two-Population Response Under Varying Connectivity Levels. Populations were connected via excitatory-excitatory connections and first modeled to a certain amount between 0-20 seconds. Connectivity was decreased to 0.03 for the next 20 seconds. Finally, connectivity was increased back to the original number.

Section 3: Network

The modeling thus far has focused on single populations and small networks. DBS is thought to directly modulate a network of brain regions (McIntyre & Hahn, 2010)**.** In the case of SCCwm-DBS, stimulation is known to modulate a network of brain regions [Mayberg, 2009]. In order to better account for stimulation effects on the brain, I extended the model to a network of brain regions to understand how and where a topologically informed network of Wilson Cowan populations may generate these transient down chirps.The Wilson Cowan populations were set up to be the same with the following parameter set: $w_{ei} = 1.5$, $w_{ie} = 1$, $w_{ii} = 0.25$, $w_{ee} = 1$, $\varphi_E = 0.125$, $\varphi_I = 0.4$, $\tau_E = 0.01$s, $\tau_I = 0.0072$s, $r_E = 0$, $r_I = 0$, $a_E = 50$, $a_I = 50$, $\theta_E = 0$, $\theta_I = 0$ (Figure 6). These parameters were set such that in unconnected to each other, the Wilson Cowan models are capable or each generating a stable oscillatory behavior. The initial excitatory/inhibitory firing populations were randomized to be within 0.25 +/- 0.05 and

0.12 +/- 0.01 respectively. Excitatory-Excitatory connections were set to 0.1 to simulate a lower impact of further away sources to the excitatory/inhibitory subpopulations within a region. Other connectivity between 0.05 and 0.3 were explored. While capable of generating transient down chirps, the ratio of time constants for excitatory/inhibitory subpopulations becomes much less than 1 and difficult to justify using experimental time constants for Glutamate and GABA actions as the connectivity between regions increased above 0.15. Furthermore, oscillations were not found in the model at connectivity above 0.19. As a simple sensitivity analysis, the model was run with a connectivity of 0.2 (Figure 7).

This network of Wilson Cowan populations showed the appearance of down chirps in certain nodes following sudden decreases in the connectivity between regions. Down chirps often occurred in regions both downstream and upstream from the location of stimulation.

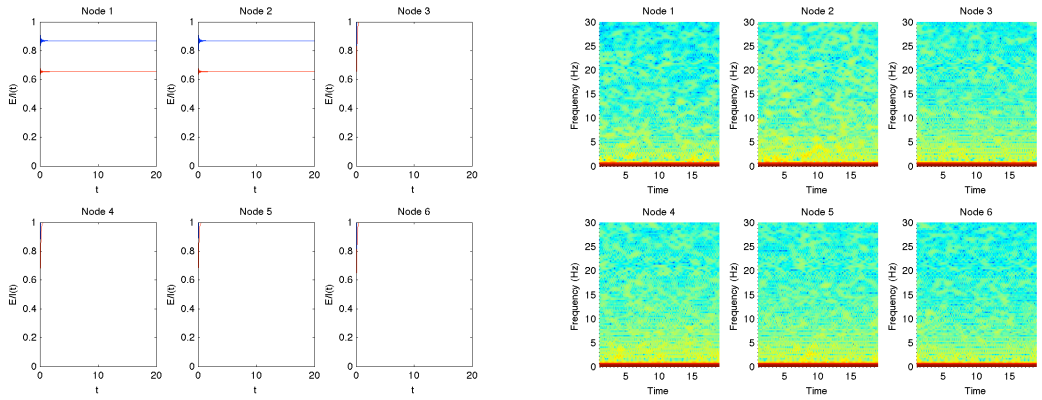

Figure 7. **Sensitivity test showing upper bound of connectivity.** Inability to generate transient down chirps after connectivity increases to 0.2. Stimulation was simulated by changing connectivity between nodes 1 and 2 to 0.

Frequency Space

Spectrogram representations of the network following a decrease in connectivity between nodes 2 and 3 showed distinctive down transient down chirps that occur in nodes 5 and 6 (Figure 8). Node 2 showed a 12 second down chirp followed by an up chirp over the course of 25 seconds.

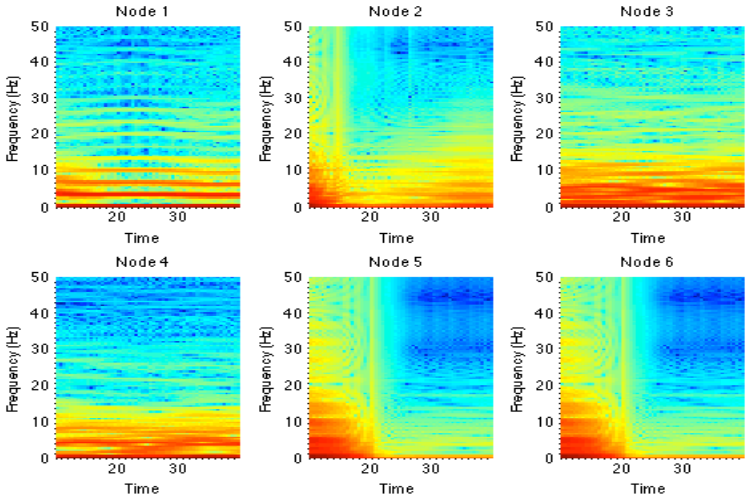

Figure 8. Spectrograms of Network Modeled Regions. Normal connectivity was assumed to be 0.25. Stimulation was simulated by changing connectivity between nodes 2 and 3 to zero.

Further simulations, taking into advantage the geometry of the model SCC circuit and utilizing biologically feasible time constants for glutamate and GABA showed the advent of chirps occurring in regions downstream and upstream of the simulated white matter tract of stimulation (Figure 9). It was found that decreasing the connectivity between nodes 2 and 3 caused the appearance of transient down chirps in the modeled left SCC (region 1).

Finally, an inhibitory connectivity was added between modeled regions as a means of exploring other possible connections not originally assumed in the model. There has been literature showing that DBS of TRD in rat models are dependent on the integrity of serotonergic systems (Hamani et al., 2010; Delaloye & Holtzheimer, 2014).

Thus, serotonin time scaled inhibitory-inhibitory and inhibitory to excitatory connections were added to study possible effects on the location of the transient down chirp appearance. It was found that this addition caused the appearance of transient down chirps in the right medial frontal regions to occur (Figure 10).

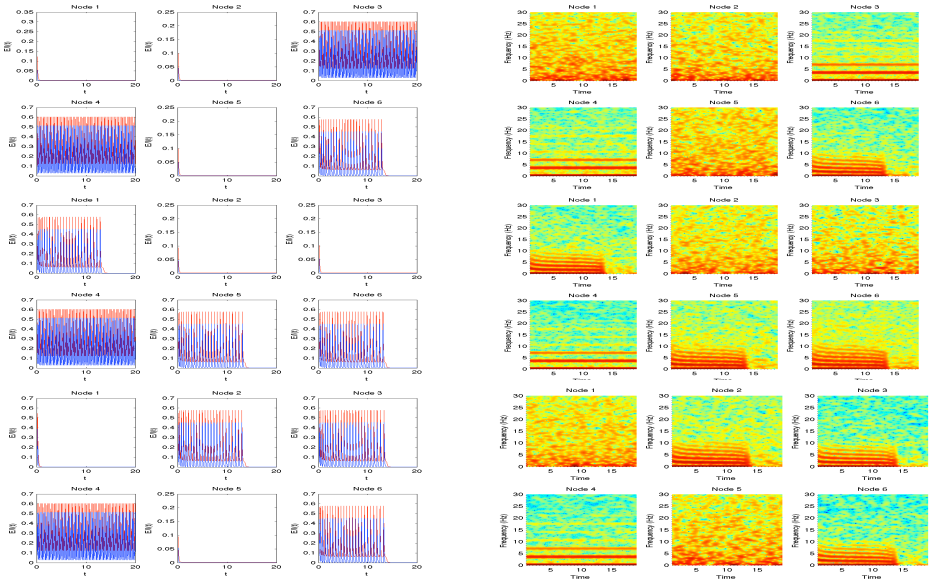

Figure 9. Time traces and Spectrograms of Network Modeled Regions. Normal connectivity was assumed to be 0.1. From top to bottom, stimulation was simulated by decreasing connectivity between nodes 1 and 2, nodes 2 and 3, and nodes 1 and 3 to 0 to represent stimulation on the uncinate fasciculus. Left panels show time course and right panels show spectrogram responses of modeled regions. 1/f base noise was added post hoc for visualization of spectrogram.

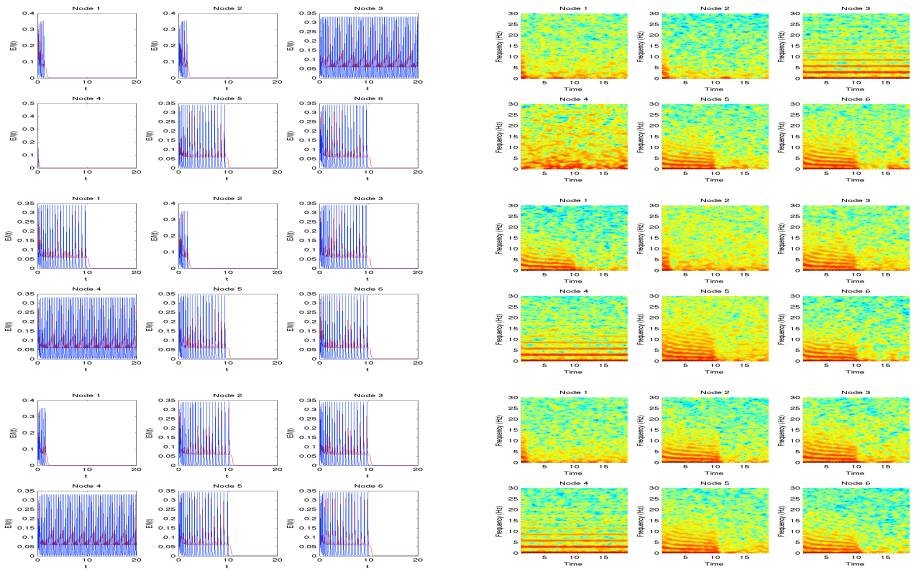

Figure 10. Time traces and Spectrograms of Network Modeled Regions with Seratonin. Normal connectivity was assumed to be 0.1. Network level inhibitory connections were added to simulate Serotonin. From top to bottom, stimulation was simulated by decreasing connectivity between nodes 1 and 2, nodes 2 and 3, and nodes 1 and 3 to 0 to represent stimulation on the uncinate fasciculus. Left panels show time course and right panels show spectrogram responses of modeled regions. 1/f base noise was added post hoc for visualization of spectrogram.

Section 4: Toolbox

Clinical investigators can greatly benefit from computational models. In strict experimental setups, precise control over variables enables direct study of pairwise variable interactions. Such a strict experimental setup is impossible in clinical populations. Computational models bridge the gap by enabling hypothesis-testing of explicit objective models in the context of clinical data. In order to make computational models more palatable to clinicians, easy-to-use interfaces and application program interfaces (API) are a critical necessity.

As a final step, I develop a MATLAB graphical user interface (GUI) to make the developed model accessible to clinical investigators. Specifically, the GUI developed was designed to enable easier exploration of the parameter space. Future integration into a set of tools capable of helping to inform and predict DBS action is a major goal.

A MATLAB graphical user interface (GUI) and toolkit was then developed to allow for ease of parameter space explorations for the model and for potential future integration into a set of tools capable of helping to inform and predict DBS action. The GUI was set up to allow for user input of Wilson Cowan parameters and displays the time course and frequency decomposition of the resulting Excitatory and Inhibitory population responses. Phase plane and Jacobian based eigenvalue portraits can be generated utilizing an analysis function within the GUI (Figure 11). Confirmation of the toolbox included comparison to the results from the previous three sections. Further verification was conducted comparing to results published in literature (Onslow, 2014; Meijer et al, 2015). An example result with a parameter as defined by literature is shown in figure 9 (Onslow,

2014). The parameters were set at $w_{ei} = 2$, $w_{ie} = 2$, $w_{ii} = 0$, $w_{ee} = 2.4$, $\varphi_E = 0.7$, $\varphi_I = 0$, $\theta_E = 1$, $\theta_I = 1$, $\tau_E = 0.0032s$, $\tau_I = 0.0032s$, $r_E = 0$, $r_I = 0$, $a_E = 4$, $a_I = 4$.

The work done here is a first step in the larger goal of enabling rapid model fitting to empirical electrophysiology. The GUI interface, combined with the model itself, can be used to quantify empirical electrophysiology in the context of excitatory and inhibitory networks.

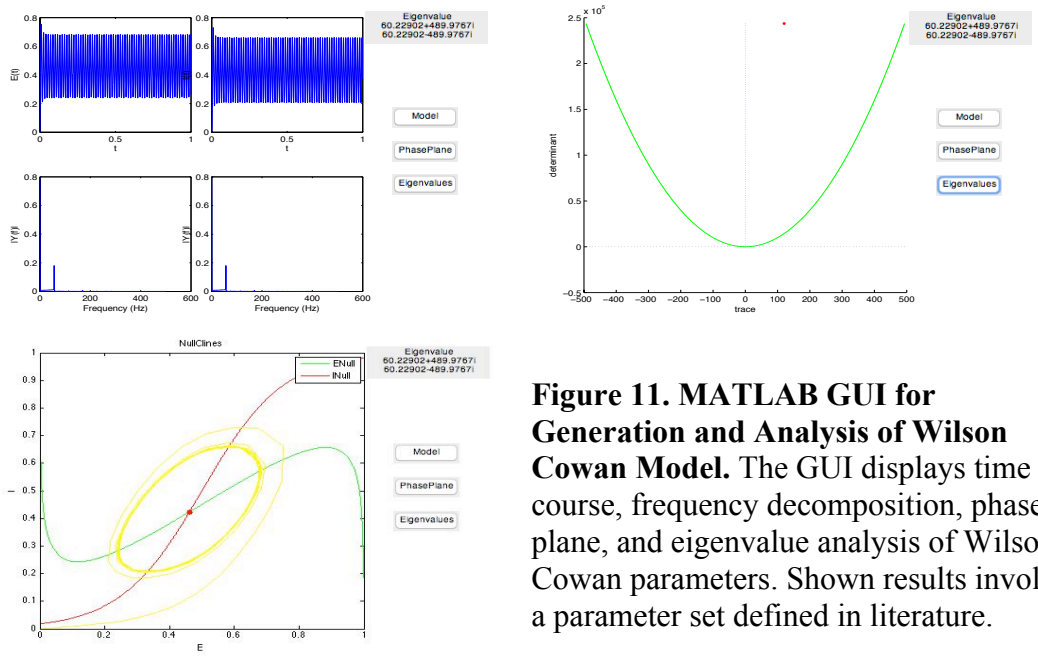

Figure 11. MATLAB GUI for Generation and Analysis of Wilson Cowan Model. The GUI displays time course, frequency decomposition, phase plane, and eigenvalue analysis of Wilson Cowan parameters. Shown results involved a parameter set defined in literature.

CHAPTER 4

DISCUSSION

Precise stimulation of white matter tracts passing through the SCC alleviated depression by an unknown mechanism. In this study, we develop a model with the intent of explaining specific oscillatory features found in empirical electrophysiology. Local field potential recordings of the SCC in DBS of SCCwm tracts utilizing implanted Medtronic PC+S neurostimulator at 130 hz frequency in clinical trials have shown the emergence of transient down chirps. Electrophysiology studies in patient populations is complicated by the lack of experimental control. Despite this limitation, hypothesis testing is possible through the use of computational models. In this thesis, I developed a computational model using basic principles of excitatory-inhibitory balance.
Utilizing a network of Wilson Cowan models informed by a network of neural regions and white matter tracts involved in DBS of SCCwm tracts in TRD patients, we were able to both generate and show that these transient down chirps may be caused at specific excitatory and inhibitory neuron population balance. Utilizing this and future expansions of this model coupled with biological constraints would allow for a noninvasive method of predicting when and under what circumstances these transient down chirps could occur and to help guide future hypothesis based clinical testing with DBS. To this end, a graphical user interface allowing for analysis and ease of testing various parameter sets was developed.

The proposed mean field model showed that transient down chirps appear when the excitatory-inhibitory phase plane trajectory reaches a homoclinic bifurcation (Figure

4). This homoclinic bifurcation is at its core a specific excitatory-inhibitory balance. This idea of an excitatory-inhibitory balance can also be seen in experiments (Chiken & Nambu, 2014) for Parkinson's disease and models for periodic stimulation (Mahmud & Vassanelli, 2016). Thus, looking at the single population phase plane alone, one could think of the transient down chirp as an intra-population response in the neuron population to reach this excitatory-inhibitory balance.

The two-population model supported this idea of intra-population response as being the primary cause of the transient down chirp. However, this model introduced a possibility of some form of inter-population mechanism behind the down chirps (figure 6). More importantly, the two-population model showed that in the simplest case, a decrease in connectivity between the two regions could cause a transient down chirp. An increase in connectivity did not produce such a response, and often times suppressed the firing of excitatory and inhibitory populations to 0 (Figure 6). This suggests that DBS of white matter tracts may cause a decrease in population connectivity, or communication, between regions directly connected by said white matter tract.

Expansion of the two-population model into the network based on the SCC circuit showed the appearance of an inter-population mechanism of transient down-chirp generation. It can be expected that in a purely intra-population response, only the regions directly connected by the stimulated white matter tract would show the transient down chirp. However, it was the down stream nodes not directly connected to the stimulated white matter tracts that showed the appearance of transient down chirps. This could possibly suggest that either the topological layout of the network or the propagation of stimulation down the network is responsible, at least in part, with the appearance of

transient down chirps. This is important because currently, clinical LFP recordings that see these transient down chirps are recorded from only the left and right SCC's. The mean field network model results shown suggest that these patterns can also be seen in both the temporal lobes and mf10's. If these transient down chirps were indicative of successful DBS treatment of TRD patients, then it would be advantageous to record from these other regions in the SCC network.

Furthermore, of the modeled neural regions, the right mF10 was the only region to not display a transient down chirp when simulating stimulation on an edge simulating the left uncinate fasciculus white matter tract. From a modeling standpoint, the node representing the mF10 has the most connections to it. It is possible that the nearby oscillations of adjacent regions in the right hemisphere are helping to stabilize the oscillation in the right mF10.

In addition, with the introduction of serotonin based inhibitory connections on top of the original assumption of glutamate based excitatory-excitatory connections, the modeled right temporal lobe more consistently displayed these transient down chirps when they appeared in the right or left modeled SCC nodes. In terms of modeling, this may be due to the extra inhibition causing the oscillations to fall down into an unstable down node region. This is relevant because research has shown that serotonin has an effect on the mechanisms of DBS of TRD in the medial frontal stimulation in rat models (Hamani et al., 2010; Delaloye & Holtzheimer, 2014). In these experiments, the depletion of serotonin lowered the efficacy of DBS. Meanwhile the SCC network model showed that with the inclusion of a serotonin based inhibitory signal in the network model, there was a definitive change in the location and appearance of transient down chirps in the

temporal and mF10 regions. While transient down chirps were not seen in these rat models, and both the modeled and current clinical DBS are focused on the SCCwm tract, the role of serotonin might have a similar mechanism of action. This further supports the need for possible future recordings from the temporal and medial frontal regions of the SCC network.

CHAPTER 5

CONCLUSION AND FUTURE WORK

Dynamical modeling of neural regions utilizing mean field neural mass models is a important first step in understanding how excitatory and inhibitory populations may be interacting to generate reproducible electrophysiological signatures found in DBS of TRD. A major implication of this work is that now that a simple Wilson Cowan model has shown to display a transient down chirp, the model can be further expanded and optimized to be used a possible future predictor for when and where transient down chirps may occur following stimulation.

Future work needs to first address fitting the model to the current LFP data recorded from the left and right SCC. This will allow for a characterization of the amount of variance in the data that can be accounted for. The model in it's current stage is not fitted to data yet, and so can only give some qualitative predictions on what the SCC network could be doing in generating the chirps. Further investigation into modeling long distance white matter tract connections should be conducted to help biologically constrain the model. The current method of utilizing a changing connectivity matrix is a first step in modeling this connection, but future work should include possible spatial features involving possibly a more detailed special representation of the modeled stimulation site. The parameter space and assumption used in this work should be further modified for relevance in an animal model or clinical setting. Furthermore, as currently the appearance of a down chirp occurs during a homoclinic bifurcation, it is very dependent on the ratio of the excitatory and inhibitory time constants. In future models or

expansions of this model, the parameter sets should be optimized for decrease dependency on the time constants themselves.

One major assumption of the modeling work detailed above was the assumption of homogeneous populations of neurons for each neural region that are exclusively Glutamate and GABA based. This assumption is a simplification that does not reflect the true biology of the neural regions modeled. To address this, the next step would be to expand the model through a dynamic causal model approach of incorporating more subpopulations of different types of neuron subpopulations within each modeled region or the virtual brain approach of applying large fields of Wilson Cowan type models to represent each neural region. Both approach have their merits and following optimization, may explain more of the variance of the original LFP data. In addition, the work shown in this thesis assumes equal initial connectivity for white matter tracts and complete symmetry between the left and right neural regions. These assumptions are simplifications that do describe the physiology in a sufficient manner, so the results here may fail to elicit dynamics that comes with increased complexity in the model. Many of these complexities can be addressed with more detailed mesoscopic neural mass models and extensions to the current model. Ultimately, the goal of these models is to given an explanation for the transient down chirp seen in the SCC LFP data sets and to explain a certain amount of variance. Thus, factors such as noise and representation of LFP from modeled population responses should be further considered in the future.

Finally, the development of a toolbox capable to conducting all of the analysis necessary for the generation and prediction of potential electrophysiological biomarkers such as the transient down chirp is an important step to informing future closed loop DBS

devices and clinical trials. The current version of the GUI described in this thesis is an early iteration of what could be a part of a larger DBS analysis toolbox. As further analysis and possible expansions to the models, as described above, are conducted, the GUI will need to be continuously updated to reflect the ongoing research.

APPENDIX A

PARAMETER SPACE EXPLORATION

Table of Select Homoclinic Bifurcations

WEE	WEI	WIE	WII	ThrE	ThrI	TAU(crit)	AE/AI
1	1.5	1	0.25	0.125	0.4	0.67641	50
1	1.5	1	0.25	0.2	0.4	0.44506	50
1	1.5	1	0.25	0.125	0.5	0.75683	50
1	1.5	1	0.25	0.1	0.4	0.81109	50
1	1.5	1	0.25	0.125	0.3	0.570596	50

Phase Plane parameter space mapping

Thresholds shift the position of the nullclines. In the bottom left figure, we notice an increase in inhibitory threshold shifts the I-nullcline right. On the bottom right figure, we noticed an increase in excitatory threshold shifts the E-nullcline down.

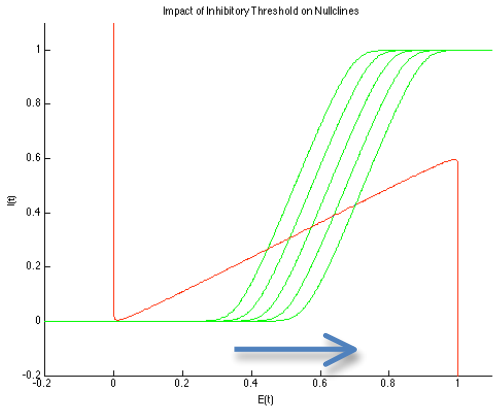

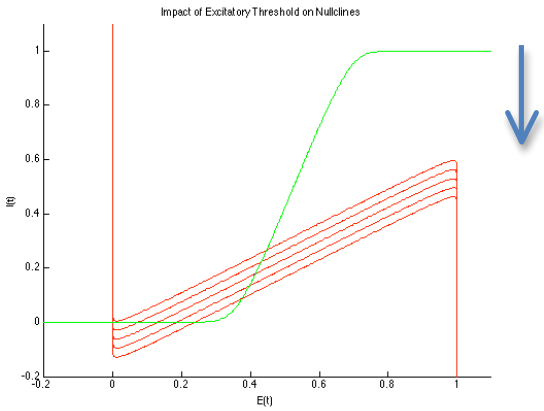

K rotates the nullclines.

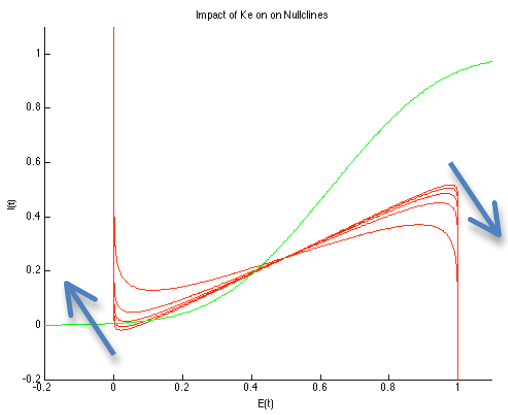

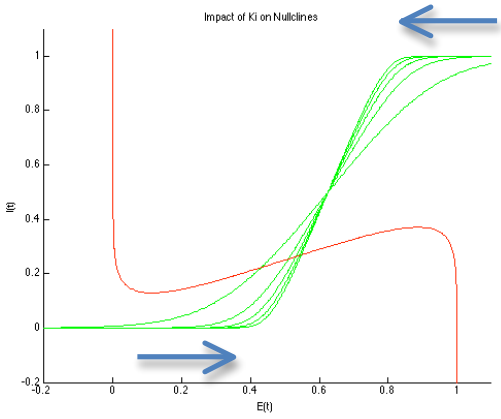

Connections between subpopulations changes curvature of nullclines.

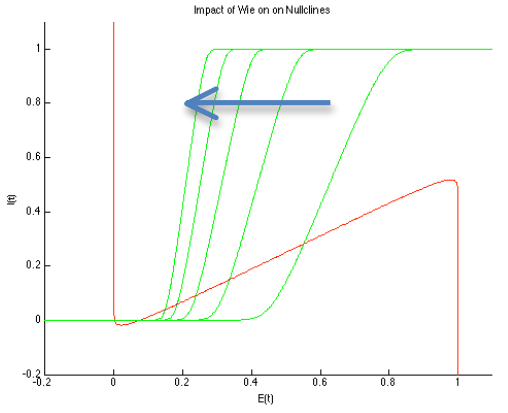

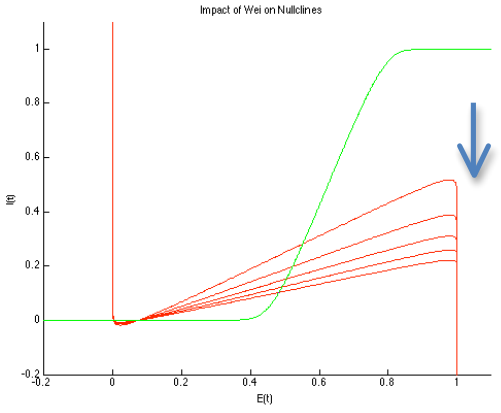

=

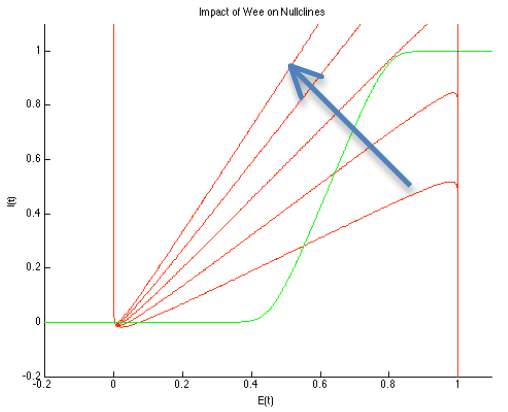

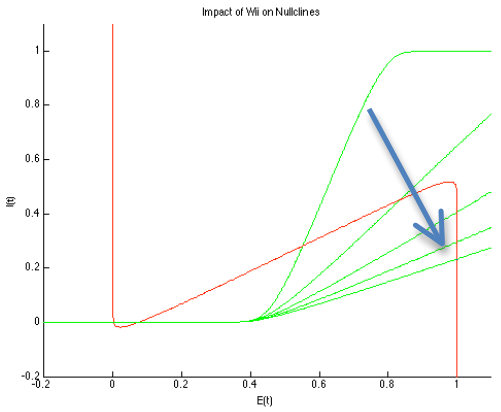

Ratio of time constant changes the trajectory of the excitatory and inhibitory populations, but does not change the nullclines themselves.

I now map out the trajectory of two different types of phase planes parameters.

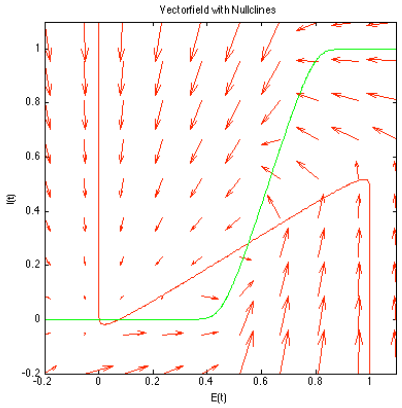

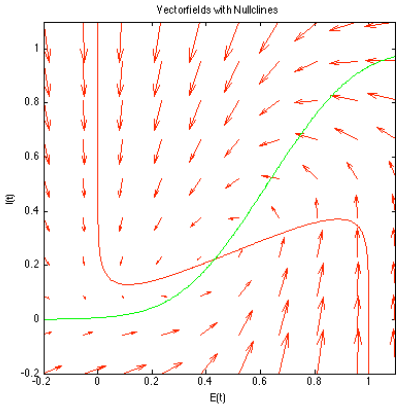

REFERENCES

[1] American Psychiatric Association. Diagnostic and Statistical Manual of Mental Disorders (DSM-5). 5th ed. Washington, DC: American Psychiatric Publishing; 2013.

[2] Bedard, C., & Destexhe, A. (2009). Macroscopic models of local field potentials and the apparent 1/f noise in brain activity. *Biophys J, 96*(7), 2589-2603. doi:10.1016/j.bpj.2008.12.3951

[3] Bédard, C., & Destexhe, A. (2015). Local Field Potential Interaction with the Extracellular Medium. In D. Jaeger & R. Jung (Eds.), *Encyclopedia of Computational Neuroscience* (pp. 1540-1547). New York, NY: Springer New York.

[4] Buzsáki, G. (2006). *Rhythms of the brain*. New York: Oxford University Press. doi:10.1093/acprof:oso/9780195301069.001.0001

[5] Chiken, S., & Nambu, A. (2014). Disrupting neuronal transmission: mechanism of DBS? *Frontiers in Systems Neuroscience*, *8*, 33. http://doi.org/10.3389/fnsys.2014.00033

[6] Computational Neuroscience Research Group@Waterloo. (n.d.). Retrieved April 23, 2017, from http://compneuro.uwaterloo.ca/research/constants-constraints/neurotransmitter-time-constants-pscs.html

[7] Delaloye, S., & Holtzheimer, P. E. (2014). Deep brain stimulation in the treatment of depression. Dialogues in Clinical Neuroscience, 16(1), 83–91.

[8] Einevoll, G. T., Kayser, C., Logothetis, N. K., & Panzeri, S. (2013). Modelling and analysis of local field potentials for studying the function of cortical circuits. *Nat Rev Neurosci, 14*(11), 770-785. doi: 10.1038/nrn3599

[9] Fava, M. (2003). Diagnosis and definition of treatment-resistant depression. *Biol Psychiatry, 53*(8), 649-659.

[10] Florin, E., & Baillet, S. (2015). The brain's resting-state activity is shaped by synchronized cross-frequency coupling of neural oscillations. *NeuroImage*, *111*, 26–35. http://doi.org/10.1016/j.neuroimage.2015.01.054

[11] Froemke, R. C. (2015). Plasticity of Cortical Excitatory-Inhibitory Balance. Annual Review of Neuroscience, 38, 195–219. http://doi.org/10.1146/annurev-neuro-071714-034002

[12] Hamani, C., Diwan, M., Macedo, C. E., Brandao, M. L., Shumake, J., Gonzalez-Lima, F., . . . Nobrega, J. N. (2010). Antidepressant-like effects of medial prefrontal cortex deep brain stimulation in rats. *Biol Psychiatry, 67*(2), 117-124. doi:10.1016/j.biopsych.2009.08.025

[13] Hopfield, J., & Tank, D. (1986). Computing with neural circuits: a model. *Science, 233*(4764), 625-633. doi: 10.1126/science.3755256

[14] Kerr, C. C., Van Albada, S. J., Neymotin, S. A., Chadderdon, G. L., Robinson, P. A., & Lytton, W. W. (2013). Cortical information flow in Parkinson's disease: a composite network/field model. *Frontiers in Computational Neuroscience*, *7*, 39. http://doi.org/10.3389/fncom.2013.00039

[15] Lewis, D. A., Glantz, L. A., Pierri, J. N., & Sweet, R. A. (2003). Altered cortical glutamate neurotransmission in schizophrenia: evidence from morphological studies of pyramidal neurons. Ann N Y Acad Sci, 1003, 102-112.

[16] Maddock, R. J., Casazza, G. A., Fernandez, D. H., & Maddock, M. I. (2016). Acute Modulation of Cortical Glutamate and GABA Content by Physical Activity. *J Neurosci, 36*(8), 2449-2457. doi:10.1523/jneurosci.3455-15.2016

[17] Mahmud, M., & Vassanelli, S. (2016). Differential Modulation of Excitatory and Inhibitory Neurons during Periodic Stimulation. Frontiers in Neuroscience, 10, 62. http://doi.org/10.3389/fnins.2016.00062

[18] Mayberg, H. S. (2009). Targeted electrode-based modulation of neural circuits for. *J Clin Invest, 119*(4), 717-725. doi:10.1172/jci38454

[19] Mayberg, H. S., Lozano, A. M., Voon, V., McNeely, H. E., Seminowicz, D., Hamani, C., . . . Kennedy, S. H. (2005). Deep brain stimulation for treatment-resistant depression. *Neuron, 45*(5), 651-660. doi: 10.1016/j.neuron.2005.02.014

[20] McCarthy, M. M., Moore-Kochlacs, C., Gu, X., Boyden, E. S., Han, X., & Kopell, N. (2011). Striatal origin of the pathologic beta oscillations in Parkinson's disease. *Proceedings of the National Academy of Sciences of the United States of America*, *108*(28), 11620–11625. http://doi.org/10.1073/pnas.1107748108

[21] McIntyre, C. C., Grill, W. M., Sherman, D. L., & Thakor, N. V. (2004). Cellular effects of deep brain stimulation: model-based analysis of activation and inhibition. *J Neurophysiol, 91*(4), 1457-1469. doi:10.1152/jn.00989.2003

[22] McIntyre, C. C., & Hahn, P. J. (2010). Network perspectives on the mechanisms of deep brain stimulation. *Neurobiol Dis, 38*(3), 329-337. doi:10.1016/j.nbd.2009.09.022

[23] Meijer, H. G., Eissa, T. L., Kiewiet, B., Neuman, J. F., Schevon, C. A., Emerson, R. G., . . . van Drongelen, W. (2015). Modeling focal epileptic activity in the Wilson-cowan model with depolarization block. *J Math Neurosci, 5*, 7. doi: 10.1186/s13408-015-0019-4

[24] Molaee-Ardekani, B., Benquet, P., Bartolomei, F., & Wendling, F. (2010). Computational modeling of high-frequency oscillations at the onset of neocortical partial seizures: From 'altered structure' to 'dysfunction'. *NeuroImage, 52*(3), 1109-1122. doi:https://doi.org/10.1016/j.neuroimage.2009.12.049

[25] Moran, R. J., Kiebel, S. J., Stephan, K. E., Reilly, R. B., Daunizeau, J., & Friston, K. J. (2007). A neural mass model of spectral responses in electrophysiology. *NeuroImage, 37*(3-3), 706-720. doi:10.1016/j.neuroimage.2007.05.032

[26] Nobler, M. S., Oquendo, M. A., Kegeles, L. S., Malone, K. M., Campbell, C. C., Sackeim, H. A., & Mann, J. J. (2001). Decreased regional brain metabolism after ect. *Am J Psychiatry, 158*(2), 305-308. doi:10.1176/appi.ajp.158.2.305

[27] Onslow, A. C. E., Jones, M. W., & Bogacz, R. (2014). A Canonical Circuit for Generating Phase-Amplitude Coupling. *PLoS ONE, 9*(8), e102591. doi: 10.1371/journal.pone.0102591

[28] Riva-Posse, P., Choi, K. S., Holtzheimer, P. E., Crowell, A. L., Garlow, S. J., Rajendra, J. K., . . . Mayberg, H. S. (2017). A connectomic approach for subcallosal cingulate deep brain stimulation surgery: prospective targeting in treatment-resistant depression. *Mol Psychiatry*. doi:10.1038/mp.2017.59

[29] Riva-Posse, P., Choi, K. S., Holtzheimer, P. E., McIntyre, C. C., Gross, R. E., Chaturvedi, A., . . . Mayberg, H. S. (2014). Defining critical white matter pathways mediating successful subcallosal cingulate deep brain stimulation for treatment-resistant depression. *Biol Psychiatry, 76*(12), 963-969. doi: 10.1016/j.biopsych.2014.03.029

[30] Sanz-Leon, P., Knock, S. A., Spiegler, A., & Jirsa, V. K. (2015). Mathematical framework for large-scale brain network modeling in The Virtual Brain. *NeuroImage, 111*, 385-430. doi:http://doi.org/10.1016/j.neuroimage.2015.01.002

[31] Soula, H., & Chow, C. C. (2007). Stochastic dynamics of a finite-size spiking neural network. *Neural Comput, 19*(12), 3262-3292. doi: 10.1162/neco.2007.19.12.3262

[32] Wilson, H. R., & Cowan, J. D. (1972). Excitatory and Inhibitory Interactions in Localized Populations of Model Neurons. *Biophysical Journal, 12*(1), 1-24.

[33] BROWN, G. L. and ROSHKO, A. "The effect of names in full upper case in numerical references," J. Fluid Mech., vol. 26, pp. 225–236, 1966.